Does the Decomposition of Peroxydicarbonates and Diacyl Peroxides Proceed in a Stepwise or Concerted Pathway?

Zhihui Gu, Yixuan Wang,† and Perla B. Balbuena*

Department of Chemical Engineering, Texas A&M University, College Station, Texas 77843

Received: September 26, 2005; In Final Form: December 16, 2005

Møller−Plesset perturbation theory and density functional theory calculations are used to study decomposition mechanisms of polymerization initiators, such as diethyl peroxydicarbonate, trifluoroacetyl peroxide, and acetyl peroxide, which possess a general structure of RC(O)OO(O)CR. It is found that the decomposition of initiators with electron-donating R groups follows two favorable stepwise pathways: a two-bond cleavage mechanism in which the O−O single bond and one of R−C bonds of [R−C(O)O−O(O)C−R] break simultaneously followed by decomposition of the R−C(O)O• radical and a one-bond cleavage mechanism in which the single O−O bond cleavage produces a carboxyl radical pair and a subsequent decomposition of the carboxyl radicals. It is also found that the initiators with electron-withdrawing R groups follow the two-bond cleavage pathway only. Geometrical and energetic analyses indicate that despite the similar structures of the peroxydicarbonates, quite different decomposition energy barriers are determined by the nature of the R groups.

1. Introduction

Organic peroxides are widely used as initiators in free-radical polymerizations, and studies on the decomposition of organic peroxides are of importance in a variety of processes.[1,2] Decompositions of diacyl peroxide and peroxydicarbonate polymerization initiators into alkyl or alkoxy radicals carried out in traditional organic solvents have been extensively studied by experimentalists.[1,3,4] The structure of peroxydicarbonates (Scheme 1) is similar to those of diacyl peroxides with a general structure of RC(O)OO(O)CR, where the R groups are alkyl for diacyl peroxides and alkoxy for peroxydicarbonates. Peroxydicarbonates are traditionally included in the diacyl peroxide category.[4] As shown in Scheme 2, three decomposition mechanisms were proposed by previous studies of diacyl peroxides and peroxydicarbonates:[1,4] (1) a single O−O bond cleavage produces a carboxyl radical pair and a subsequent decomposition of the carboxyl radicals; (2) a stepwise pathway including two steps: an initial two-bond cleavage to a carboxyl radical, an alkyl (or alkoxy) radical and CO_2, followed by decomposition of the carboxyl radical; (3) a concerted three-bond cleavage to an alkyl (or alkoxy) radical pair and two CO_2 molecules. The decarboxylation of the intermediate carboxyl radicals such as aroyloxy radicals has been studied by optical detection[5,6] and EPR spectroscopy.[7] These studies showed a decomposition rate of 10^7 s^{-1} with an approximate activation energy of 8−9 kcal/mol. Recent studies on the decarboxylation of carboxyl radicals with general structure RC(O)O by means of femtosecond time resolution UV pump−VIS/near-IR spectroscopy and quantum chemical methods have been reported.[8−12]

For the overall decomposition of peroxydicarbonate and peroxide initiators, the observed kinetics is primarily first order.[1,4,13] For example, the decomposition of diethyl peroxydicarbonate (DEPDC) was found to be first order with a measured activation energy of 31.58 ± 1.91 kcal/mol in supercritical CO_2 solvent.[12] Experimental studies usually can only give us overall decomposition reaction kinetics such as the activation energy of decomposition, and it may be difficult to distinguish details of the above-mentioned reaction mechanisms. Theoretical studies offer alternative means of exploring detailed decomposition reaction pathways at a molecular level, providing the activation energy of each decomposition step.

SCHEME 1. Molecular Structure of DEPDC (diethyl peroxydicarbonate), TFAP, and AP (diacyl peroxides) Initiators[a]

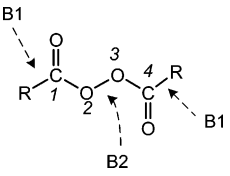

[a] R = C_2H_5O for DEPDC, R = CF_3 for TFAP, and R = CH_3 for AP.

In addition, experiments have shown that solvents affect both the decomposition rate constant and the peroxide initiator efficiency. Perfluorinated diacyl peroxide, for instance, has a higher decomposition rate in supercritical CO_2 with an activation energy lower by 6 kcal/mol as compared with other solvents.[14] Such effects may be caused by solvent properties such as polarity and viscosity. To theoretically investigate the solvent effects on decomposition, the first step is to develop a better understanding of the decomposition mechanism of the peroxide initiators. However, to the best of our knowledge, no theoretical studies have been reported on the decomposition mechanism of peroxydicarbonates. In this paper, we present Møller−Plesset perturbation theory[15] and density functional theory (DFT) calculations of the decomposition of DEPDC, trifluoroacetyl peroxide (TFAP), and acetyl peroxide (AP) (structures shown

* To whom correspondence should be addressed. E-mail: balbuena@tamu.edu.

† Current address: Department of Natural Science, Albany State University, 504 College Drive, Albany, Georgia 31705.

10.1021/jp055472k CCC: $33.50
Published on Web 02/01/2006

SCHEME 2. Previously Proposed Thermal Decomposition Mechanisms for Peroxydicarbonates and Diacyl Peroxide Initiators

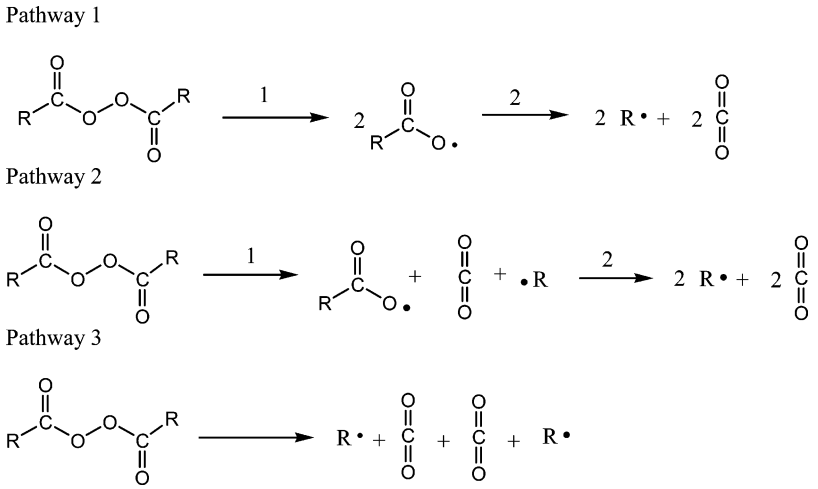

TABLE 1: Calculated Bond Lengths (Å) and D and A Angles (deg) of DEPDC, TFAP, and AP (nomenclature given in Scheme 1)

molecule	B1(R−C1/C4)	B2(O2−O3)	D(C1−O2−O3−C4)	A(O−C−O)
DEPDC	1.33	1.43	−85.62	126
TFAP	1.55	1.44	−87.17	127
AP	1.51	1.44	−83.21	124

in Scheme 1) including their decomposition pathways and thermodynamics for the involved elementary decomposition reactions.

2. Computational Details

The Gaussian03 Rev C.02 program package[16] was employed for all calculations. The density functional used is the hybrid exchange functional Becke3[17] in combination with the LYP correlation functional,[18] referred to as B3LYP. The ab initio MP2 method[19−22] is the Møller−Plesset second-order correlation energy correction to the Hartree−Fock approximation. The reactants, intermediates, transition states, and products along the decomposition pathway were optimized with both B3LYP and MP2 methods. Calculated minima have no imaginary frequencies, whereas the transition states possess only one imaginary frequency. Intrinsic reaction coordinate[23,24] calculations were performed for all transition states to confirm their identification as true transition states connecting reactants and products. Relative energies were calculated with zero-point energy correction; the enthalpies, entropies, and Gibbs free energies were calculated at 298.15 K.

3. Results and Discussion

3.1. Geometrical Analysis of RC(O)OOC(O)R Initiators. Structural analysis of polymerization initiators are based on the DFT-optimized structures, shown in Figure 1 for DEPDC, TFAP, and AP. The R groups influence the structure of the central section of the diacyl peroxides and diethyl peroxydicarbonate, as illustrated in Table 1 for the R−C1/C4 and O2−O3 bond lengths and for the C1−O2−O3−C4 dihedral and O−C−O angles (nomenclature of Scheme 1). The estimated stretching frequencies of the O−O bond are 1103, 921, and 952 cm^{-1} (B3LYP/6-31G(d) level, no scaling) for DEPDC, TFAP, and AP, respectively, indicating that the C_2H_5O group makes the O−O bond slightly stronger than those of AP and TFAP although the bond lengths are almost the same. The bond connecting the ethoxy group with C1/C4 in DEPDC, i.e., H_5C_2O−C1/C4, is 0.01 Å shorter than those (F_3C/H_3C−C1/C4) of TFAP and AP. These differences in bond strengths may be partially responsible for the difference in decomposition activation energies, as discussed in a later section. The dihedral angle (C1−O2−O3−C4) of each initiator provides an indication of the effect of the R group on the structures of DEPDC, TFAP, and AP. Comparing TFAP with AP, it is observed that fluorination increases the dihedral angle of the central section and destabilizes the B1 bond. Therefore, the activation energy for the decomposition of TFAP may be lower than that of AP.

3.2. Decomposition Pathways. Despite many efforts, which included a number of different initial structures for the transition states, we failed to locate the transition state of pathway 3 (Scheme 2), the three-bond concerted cleavage reaction pathway, with the current DFT and MP2 methods. Instead, with both DFT and MP2 methods, a transition state (TS2) for the decomposition from the initiators directly to one carboxyl radical, one alkoxy/alkyl radical, and one CO_2 molecule (step 1 in pathway 2, Scheme 2) was obtained for all three initiators (DEPDC, TFAP, and AP). Also, the transition state (TS3) for the decomposition

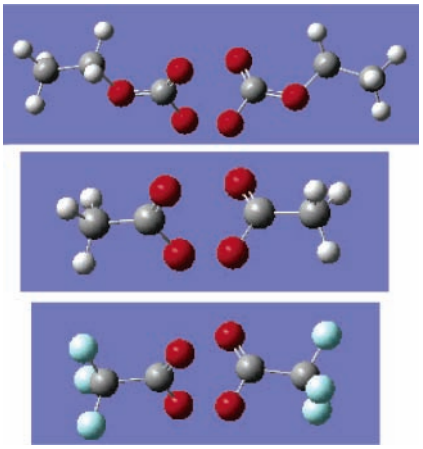

Figure 1. Optimized structures (B3LYP/6-31G(d)) of DEPDC, TFAP, and AP. Geometrical parameters are given in Table 1.

SCHEME 3. Thermal Decomposition Mechanisms for Peroxydicarbonate and Diacyl Peroxide Initiators Based on MP2 Calculations[a]

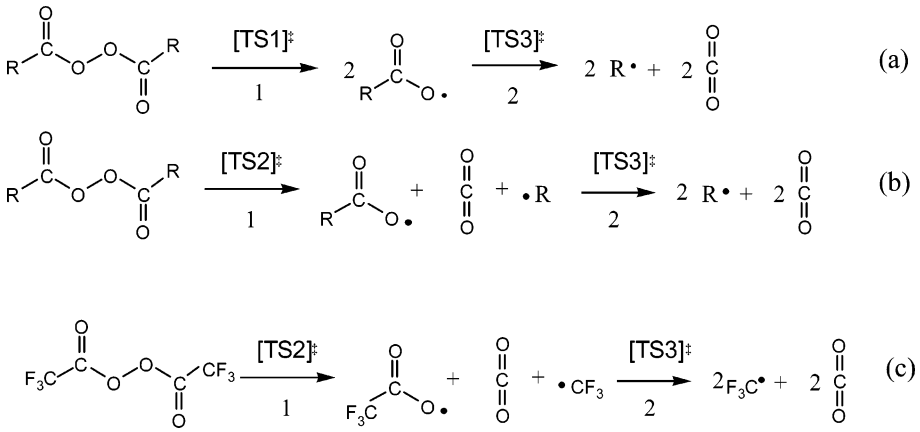

[a] DEPDC and AP decomposition pathways: (a) one-bond cleavage mechanism and (b) two-bond cleavage mechanism (R = C_2H_5O for DEPDC; R = CH_3 for AP). (c) TFAP decomposition pathways: two-bond cleavage mechanism.

TABLE 2: Calculated Activation Parameters of Transition States (TS1, TS2, TS3) for DEPDC Decomposition by MP2 and DFT Methods with Different Basis Sets[a]

method	D$E^{\ddagger}$	$\Delta H^{\ddagger}$	$\Delta G^{\ddagger}$
one-bond cleavage mechanism/TS1			
MP2/6-31G(d)	43.99	44.54	42.48
two-bond cleavage mechanism/TS2			
MP2/6-31G(d)	45.00	45.64	43.78
B3LYP/6-31G(d)	59.92	60.79	58.12
B3LYP/6-311+G(2d,p)	57.52	58.49	55.39
intermediate radical decomposition/TS3			
MP2/6-31G(d)	13.64	13.66	13.47
B3LYP/6-31G(d)	13.09	13.25	12.03
observed experimental overall decomposition activation parameter[12]			
solvent: CO_2	31.58 ± 1.91		

[a] Original calculation data are shown in Table 8. Energies in kcal/mol.

TABLE 3: Calculated Activation Parameters of Transition States (TS1, TS2, TS3) for AP Decomposition by MP2 and DFT Methods with Different Basis Sets[a]

method	$\Delta E^{\ddagger}$	$\Delta H^{\ddagger}$	$\Delta G^{\ddagger}$
one-bond cleavage mechanism/TS1			
MP2/6-31G(d)	30.50	31.22	29.24
two-bond cleavage mechanism/TS2			
MP2/6-311+G(2d,p)	27.39	28.05	26.59
B3LYP/6-31G(d)	45.34	46.13	43.92
B3LYP/6-311+G(2d,p)	40.27	41.06	39.00
intermediate radical decomposition/TS3			
MP2/6-31G(d)	9.44	9.37	9.94
B3LYP/6-31G(d)	5.33	6.00	4.08
observed experimental overall decomposition activation parameter[25]			
solvent: CO_2[b]		28.4	27.4
solvent: C_6H_{12}[c]		31.4	27.5
gas phase[d]		28.8	27.3

[a] Original data shown in Table 9. Energies in kcal/mol. [b] Density 0.83 g/mL. [c] Original data from ref 27. [d] Original data from ref 26.

of intermediate carboxyl radicals into alkoxy/alkyl radicals and CO_2 was obtained (step 2 in pathways 1 and 2, Scheme 2) by both DFT and MP2 methods. On the other hand, for the one-bond cleavage mechanism in which initiators decompose into one pair of intermediate carboxyl radicals (step 1 in pathway 1, Scheme 2), the transition states (TS1) were obtained using the MP2 method only, for DEPDC and AP decompositions.

Thus, two possible calculated decomposition pathways for DEPDC and AP are shown in Scheme 3: one is the one-bond cleavage mechanism in which the O−O bond homolytic cleavage produces a carboxyl radical pair and a subsequent decomposition of the carboxyl radicals; another is that where the initiators first decompose to produce a carboxyl radical, an alkoxy/alkyl radical, and one CO_2 molecule after the O−O and one of R−C bonds break simultaneously, and then the intermediate carboxyl radical further decomposes, yielding another alkoxy/alkyl radical and CO_2. These calculated decomposition processes agree with the proposed decomposition pathways 1 and 2 in Scheme 2 for DEPDC and AP, suggesting the one- or two-bond cleavage mechanisms shown in Scheme 3. For the decomposition of TFAP, only the two-bond cleavage mechanism was confirmed by the DFT and MP2 calculations. A reported mechanism of thermal decomposition of bis(perfluoro-2-*N*-propoxyprionyl) peroxide[20] without an initial geminate carboxyl radical pair is in agreement with this calculation.

Table 2 shows the activation parameters of DEPDC decomposition corresponding to TS1 in the one-bond cleavage, TS2 in the two-bond cleavage mechanism, and TS3 in the intermediate radical decomposition. The activation energy of TS2 obtained from B3LYP/6-31g(d) (59.92 kcal/mol) is higher than that (45.00 kcal/mol) obtained from MP2/6-31g(d); the latter is closer to the experimental overall activation energy of 31.58 ± 1.91 kcal/mol.[12] The DFT results with a larger basis set such as 6-311+G(2d,p) yield a slightly lower activation energy of 57.52 kcal/mol but still much higher than the experimental value. From this point of view, MP2 gives a better prediction than DFT for the DEPDC decomposition study. On the other hand, the TS1 activation free energy of 42.48 kcal/mol (MP2/6-31g(d)) is similar to the TS2 activation free energy of 43.78 kcal/mol (MP2/6-31g(d)), suggesting that both the O−O one-bond cleavage and the two-bond cleavage mechanisms are favorable. From Table 2, the TS3 activation free energy of 13.67 kcal/mol (MP2/6-31g(d)) is much smaller than those of TS1 and TS2, which reveals that the first step is the rate-determining step in both pathway 1 and pathway 2.

The AP decomposition activation parameters are reported in Table 3. Similar to the DEPDC decomposition case, the MP2 activation energies for TS1 and TS2 are lower than those obtained by DFT. Again, DFT with a larger basis set yields lower TS2 activation parameters; however, the values do not agree with the experimental ones.[25] In addition, the DFT method cannot predict the transition state for one-bond cleavage for AP decomposition.

TABLE 4: Calculated Activation Parameters of Transition States (TS1, TS2, TS3) for TFAP Decomposition by MP2 and DFT Methods with Different Basis Sets[a]

method	$\Delta E^{\ddagger}$	$\Delta H^{\ddagger}$	$\Delta G^{\ddagger}$
two-bond cleavage mechanism/TS2			
MP2/6-31G(d)	27.35	27.82	26.48
B3LYP/6-31G(d)	32.83	33.61	31.19
B3LYP/6-311+G(2d,p)	29.24	29.94	27.83
intermediate radical decomposition/TS3			
MP2/6-31G(d)	10.07	10.10	10.06
B3LYP/6-31G(d)	3.53	3.42	4.07
observed experimental overall decomposition activation parameter[25]			
solvent: CO_2[b]		20.8 ± 0.2	25.4
solvent: $CF_2ClCFCl_2$[c]		25.8	25.6

[a] Original data shown in Table 10. Energies in kcal/mol. [b] Density 0.87 g/mL. [c] Original data from ref 26.

Comparing the MP2 activation parameters of TS3 with those of TS1 and TS2, it is observed that the intermediate radical decomposition is much faster than the O−O one-bond cleavage and two-bond cleavage reactions. The TS1 activation parameters such as the activation free energy (29.24 kcal/mol, MP2/6-31g(d)) and the TS2 activation free energy (26.59 kcal/mol, MP2/6-311+g(2d,p)) agree very well with the experimental overall decomposition activation free energy of 27.4 kcal/mol in supercritical CO_2 solution.[25] Therefore, it is concluded that the AP decomposition may proceed via the one-bond or the two-bond cleavage mechanism.

In contrast to the DEPDC and AP cases, only the two-bond cleavage transition state for the TFAP decomposition process was found by both DFT and MP2 methods. The MP2 activation parameters of TS2 shown in Table 4 (such as the activation free energy of 26.48 kcal/mol) agree with experimental values (activation free energy of 25.4 kcal/mol);[25] such agreement is slightly better than that given by the DFT method (27.83 kcal/mol, B3LYP/6-311+g(2d,p)). The MP2 activation parameters of TS3 (such as the activation free energy of 10.06 kcal/mol) are much smaller than those of TS2. Therefore, the TFAP decomposition follows only the two-bond cleavage mechanism, and the rate-determining step is the two-bond cleavage.

Analyzing the structure of these initiator decomposition processes, it is observed that the two initiators with electron-donating groups (CH_3 in AP, C_2H_5O in DEPDC) follow both the one-bond and the two-bond cleavage pathways, whereas TFAP having an electron-withdrawing group (CF_3) follows only the two-bond cleavage pathway, which indicates that the electron-withdrawing group destabilizes the R−C1/C4 bonds so that one of the R−C1/C4 bonds readily breaks simultaneously with the O−O bond cleavage. In DEPDC and AP, the electron delocalization on the carboxyl group caused by the electron-donating group makes the R−C1/C4 bonds stronger so that the one-bond cleavage is favorable. However, because the R−C1/C4 bond is not enough strong, the two-bond cleavage pathway also exists. In both DEPDC and AP decompositions, the activation parameters of TS1 and TS2 are similar; for example, the activation free energies of O−O and two-bond cleavage are 42.48 and 43.78 kcal/mol, respectively, in DEPDC and 29.24 and 26.59 kcal/mol in AP, respectively. These similarities of the activation parameters are due to the extent of B1 and B2 bond cleavage in different transition states. Figures 2 and 3 show the transition states of TS1 and TS2 in DEPDC, AP, and TFAP cases by MP2 method, and their geometrical parameters are reported in Table 5.

The MP2-calculated activation energy parameters of AP and TFAP are in good agreement with the experimental values. The disagreement between calculation and experimental results for DEPDC should be explored in more detail. The DEPDC decomposition kinetics was studied experimentally in supercritical CO_2.[12] It was assumed that the eventual products would be CO_2 and ethoxy radical. The reported activation energy of the decomposition is 31.58 ± 1.91 kcal/mol, and it was found that the solvent pressure has no effect on the rate constant.[12] On the basis of the present MP2 calculations, the activation energies of the elementary first steps in pathways 1 and 2 are 45.00 and 43.99 kcal/mol, respectively; thus, a difference of more than 10 kcal/mol with respect to the experimental results. Adding diffuse and polarization functions to the basis set in the MP2 calculations may yield lower calculated activation parameters based on the DFT results shown in Table 2. On the other hand, in the experiments the kinetics is evaluated on the basis of the addition of a radical scavenger. Since two different radicals (product radical and intermediate radical) are suggested by the calculated mechanism, such measurements would be conditioned by the affinity of the scavenger to each of the radicals. A third effect is that of the supercritical CO_2 solvent, which we plan to include in future MP2 calculations.

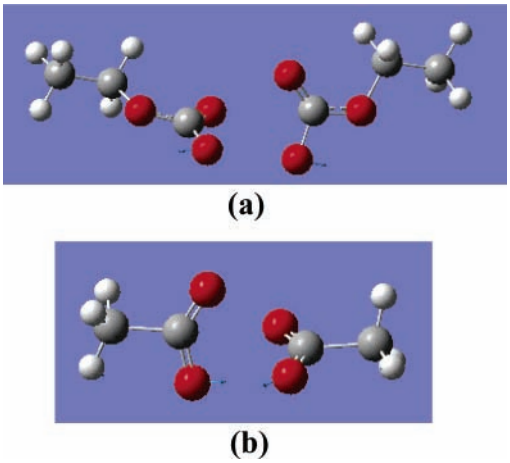

Figure 2. TS1 transition states obtained with MP2/6-31G(d) method: (a) DEPDC, (b) TFAP, (c) AP.

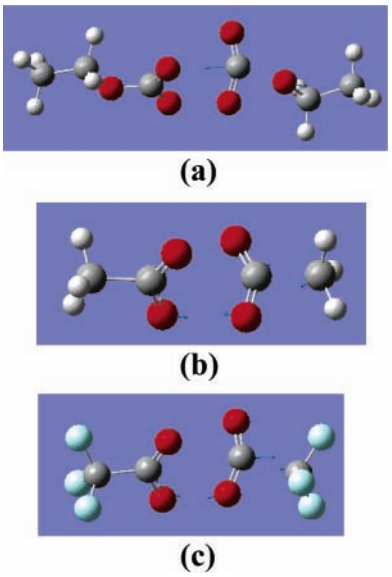

Figure 3. TS2 transition states; a and c obtained with MP2/6-31G(d) and b with MP2/6-311+g(2d,p): (a) DEPDC, (b) AP, (c) TFAP.

3.3. R Group Effects on Transition States and Activation Parameters. Table 6 shows the comparison of activation free energies of TS1, TS2, and TS3 for DEPDC, AP, and TFAP,

TABLE 5: Calculated Geometrical Parameters (B1 and B2 distances in Å, D and A angles in deg) of Reactants and Transition States for DEPDC, AP, and TFAP by MP2/6-31g(d)

		B1(R−C1/C4)	B2(O2−O3)	D(C1−O2−O3−C4)	A(O−C−O)
initiator	DEPDC	1.33	1.45	−80.64	126
	AP	1.50	1.45	−78.17	124
	TFAP	1.54	1.45	−81.72	127
TS1	DEPDC	1.34	2.48	−69.26	126
	AP	1.59	2.30	−80.88	136
TS2	DEPDC	1.69	2.05	−74.46	155
	AP[a]	1.68	2.21	−74.50	141
	TFAP	1.84	1.96	−64.29	151

[a] Calculated with MP2/6-311+G(2d,P).

TABLE 6: Comparison of Activation Free Energies of TS1, TS2, and TS3 among DEPDC, AP, and TFAP by MP2/6-31g(d)[a]

	TS1	TS2	TS3
DEPDC	42.48	43.78	13.47
AP	29.24	26.59[b]	11.11
TFAP		26.48	10.06

[a] Energy unit is kcal/mol. [b] Calculated with MP2/6-311+g(2d,p).

and the geometries of related transition states are reported in Table 5. For the O2−O3 one-bond cleavage mechanism, comparing TS1 of DEPDC with that of AP, it is concluded that the presence of the C_2H_5O groups of DEPDC are responsible for the higher activation free energy of 42.48 kcal/mol with respect to that of AP (29.24 kcal/mol) and also induce a higher extent of O2−O3 bond cleavage in the transition state than that found in AP.

For TS2, in the first decomposition step of the two-bond mechanism, the O2−O3 and one of R−C1/C4 bonds break simultaneously. The DEPDC O2−O3 distance in TS2 is 2.05 Å longer than that (1.96 Å) of TFAP (Table 5) and the elongation of B1(R−C1/C4) in DEPDC from 1.33 (reactant, DEPDC) to 1.69 Å (TS2, DEPDC) is 0.36 Å longer than that of B1 (0.30 Å) in TFAP. Besides, the DEPDC energy barrier for TS2 is 43.78 kcal/mol, which is much higher than that of TFAP, 26.48 kcal/mol. These results suggest that the activation energies and the extent of bond cleavage of the first decomposition steps of pathways 1 and 2 are closely related to the nature of the R groups. The C_2H_5O group in DEPDC yields the highest energy barrier, which is consistent with the above structural analysis, indicating that the B1 bond in DEPDC is stronger than those of AP and TFAP. The electron delocalization over the carboxyl group in DEPDC strongly stabilizes the reactant, so that the C_2H_5O−C1/C4 bond is not so easy to be decomposed. Comparing the TS2 activation energy of TFAP with that of DEPDC, CF_3 destabilizes the B1 bond of TFAP and decreases the decomposition energy barrier because of the strong electron-attracting character of the CF_3 group.

The second step in pathways 1 and 2 is the carboxyl radical decomposition into alkoxy/alkyl radical and CO_2. Activation free energies of TS3 (Table 6) show that the effects of the R groups on the activation energies of step 2 in both pathways 1 and 2 follow the same trend as that in step 1. The decarboxylation energy barriers are 13.47, 11.11, and 10.06 kcal/mol for the $C_2H_5OC(O)O$, $H_3CC(O)O$, and $F_3CC(O)O$ intermediate radicals, respectively. Figure 4 shows the structures of intermediate radicals, and their decarboxylation transition states are displayed in Figure 5. Analyzing the transition-state geometries of TS3 during the decarboxylation, it is observed that the main reaction coordinates are the elongation of the R−CO_2 bond length, the increase of the O−C−O angle in CO_2, and the decrease of the C═O bond length. Table 7 lists these changes for intermediate radicals and transition states.

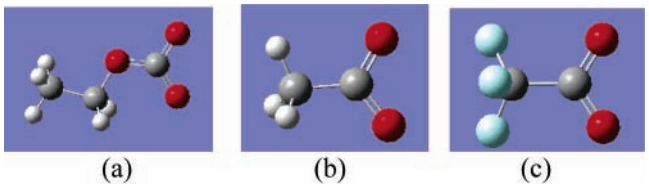

Figure 4. Structures of intermediate radicals obtained with MP2/6-31G(d): (a) $C_2H_5OC(O)O$, (b) $H_3CC(O)O$, (c) $F_3CC(O)O$.

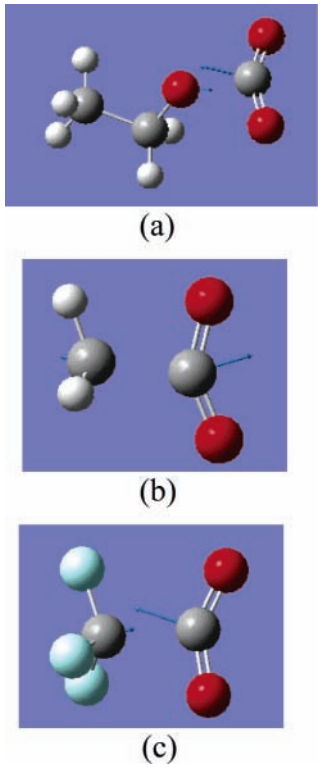

Figure 5. TS3 transition states obtained with MP2/6-31G(d): (a) $C_2H_5OC(O)O$, (b) $H_3CC(O)O$, (c) $F_3CC(O)O$.

TABLE 7: Geometrical Parameters of Intermediate Radicals (B3 distances in Å, A angles in deg) and Corresponding Transition States of TS3 Calculated with MP2/6-31G(d)

	B3 (R−CO_2)		A (O−C−O) (CO_2)	
	radical	TS3	radical	TS3
$C_2H_5OC(O)O$	1.34	1.67	121	151
$H_3CC(O)O$	1.49	1.70	110	144
$F_3CC(O)O$	1.52	1.74	113	145

In summary, according to the current MP2 calculations, the decompositions of the peroxydicarbonate and diacyl peroxides take place via the reaction pathways shown in Scheme 3 and the difference in activation energies in the two pathways is due to the influence of their respective R groups. The calculated

TABLE 8: Calculated Energies (E+ZPE), Enthalpies (*H*), and Free Energies (*G*) in Hartrees for DEPDC and Its Decomposition Transition States and Intermediate Radicals Using MP2 and DFT Methods with Different Basis Sets

		E+ZPE	H	G
B3LYP/6-31g(d)	DEPDC	−685.769110	−685.754829	−685.811137
	TS2	−685.673614	−685.657950	−685.718511
B3LYP/6-311+g(2d,p)	DEPDC	−685.999413	−685.985072	−686.041515
	TS2	−685.907754	−685.891866	−685.953246
MP2/6-31g(d)	DEPDC	−683.802864	−683.788767	−683.844527
	TS1	−683.732764	−683.717779	−683.776832
	TS2	−683.731154	−683.716035	−683.774754
B3LYP/6-31g(d)	$C_2H_5OC(O)O$	−342.868622	−342.861189	−342.900259
	TS3	−342.847766	−342.840066	−342.881082
B3LYP/6-311+g(2d,p)	$C_2H_5OC(O)O$	−342.986025	−342.978585	−343.017584
	TS3	−342.967506	−342.959730	−343.000535
MP2/6-311+g(2d,p)	$C_2H_5OC(O)O$	−342.140502	−342.133130	−342.171741
	TS3	−342.119240	−342.111808	−342.150913
MP2/6-31g(d)	$C_2H_5OC(O)O$	−341.863260	−341.855891	−341.894643
	TS3	−341.841520	−341.834113	−341.873175

TABLE 9: Calculated Energies (E+ZPE), Enthalpies (*H*), and Free Energies (*G*) in Hartrees for AP and Its Decomposition Transition States and Intermediate Radicals Using MP2 and DFT Methods with Different Basis Sets

		E+ZPE	H	G
B3LYP/6-31g(d)	AP	−456.766561	−456.756520	−456.801729
	TS2	−456.694305	−456.683002	−456.731736
B3LYP/6-311+g(2d,p)	AP	−456.922713	−456.958116	−456.958116
	TS2	−456.858540	−456.847202	−456.895960
B3LYP/6-311+g(2df,2pd)	AP	−456.938780	−456.928707	−456.974254
	TS2	−456.874506	−456.863170	−456.911927
B3LYP/6-311++g(3d,p)	AP	−456.928065	−456.917997	−456.963457
	TS2	−456.864560	−456.853247	−456.902008
MP2/6-311+g(2d,p)	AP	−455.831588	−455.821656	−455.866350
	TS2	−455.787932	−455.776959	−455.823979
MP2/6-31g(d)	AP	−455.466868	−455.456977	−455.501520
	TS1	−455.418270	−455.407222	−455.454924
B3LYP/6-31g(d)	$CH_3C(O)O$	−228.363432	−228.358810	−228.389997
	TS3	−228.354938	−228.349250	−228.383500
B3LYP/6-311+g(2d,p)	$CH_3C(O)O$	−228.443990	−228.438516	−228.472180
	TS3	−228.437245	−228.431629	−228.465584
MP2/6-311+g(2d,p)	$CH_3C(O)O$	−227.880706	−227.875320	−227.908831
	TS3	−227.865662	−227.860385	−227.892987
MP2/6-31g(d)	$CH_3C(O)O$	−227.698065	−227.692688	−227.726142
	TS3	−227.681068	−227.675783	−227.708440

TABLE 10: Calculated Energies (E+ZPE), Enthalpies (*H*), and Free Energies (*G*) in Hartrees for TFAP and Its Decomposition Transition States and Intermediate Radicals Using MP2 and DFT Methods with Different Basis Sets

		E+ZPE	H	G
B3LYP/6-31g(d)	TFAP	−1052.203373	−1052.189591	−1052.246977
	TS2	−1052.151062	−1052.136035	−1052.197275
B3LYP/6-311+g(2d,p)	TFAP	−1052.574996	−1052.561226	−1052.618225
	TS2	−1052.528399	−1052.513511	−1052.573865
MP2/6-31g(d)	TFAP	−1049.634903	−1049.621256	−1049.678428
	TS2	−1049.591315	−1049.576915	−1049.636225
B3LYP/6-31g(d)	$CF_3C(O)O$	−526.080595	−526.073456	−526.112961
	TS3	−526.075259	−526.068297	−526.107380
B3LYP/6-311+g(2d,p)	$CF_3C(O)O$	−526.268588	−526.261430	−526.301726
	TS3	−526.262952	−526.255976	−526.295235
MP2/6-31g(d)	$CF_3C(O)O$	−524.781703	−524.774678	−524.814151
	TS3	−524.765643	−524.758579	−524.798123

activation parameters of the rate-determining steps agree with the experimental overall decomposition activation parameters for AP and TFAP. The DFT method did not produce accurate results for these initiator decomposition cases.

4. Conclusions

The MP2 method seems to be much more accurate than DFT for prediction of decomposition mechanisms for DEPDC, TFAP, and AP. On the basis of our present MP2 calculation results, two possible pathways are suggested for the peroxydicarbonate or diacyl peroxide initiators with electron-donating R groups: one is the stepwise one-bond cleavage pathway in which the O−O bond cleavage produces a carboxyl radical pair which is the rate-determining step and then a subsequent decomposition of the carboxyl radicals; the other one is a two-bond cleavage pathway in which the initiators decompose first to a carboxyl radical, CO_2, and an alkoxy/alkyl radical via simultaneous cleavage of the O−O and R−C bonds, and this is the rate-determining-step. The produced carboxyl radical then decomposes, yielding another alkoxy/alkyl radical and CO_2. For the initiators with an electron-withdrawing R group such as TFAP, the MP2 method suggests the two-bond cleavage mechanism only. The R group influences the structure of initiators and determines the strength of the O−O and R−C bonds due to

their effect on electron distribution. Electron-donating R groups make stronger O−O bonds, corresponding to higher activation energies, whereas electron-withdrawing R groups destabilize the O−O bond and cause lower activation energies.

Acknowledgment. This work was supported by the National Science Foundation. Discussions with Prof. George Roberts and Prof. Keith Gubbins are gratefully acknowledged. Supercomputer time is provided by National Energy Research Scientific Center, NERSC.

References and Notes

(1) Fujimori, K. Diacyl Peroxides. In *Organic Peroxides*; Ando, W., Ed.; Wiley: New York, 1992; pp 319−385.

(2) Sawaki, Y. Peroxy acids and peroxy esters. In *Organic peroxides*; Ando, W., Ed.; Wiley: New York, 1992; pp 425−477.

(3) Brandrup, J.; Immergut, E. H.; Grulke, E. A. *Polymer Handbook*; Wiley: New York, 1999.

(4) Hiatt, R. Acyl peroxides. In *Organic peroxides*; Swern, D., Ed.; Wiley: New York, 1970; pp 801−929.

(5) Chateauneuf, J.; Lusztyk, J.; Ingold, K. U. Spectroscopic and kinetic characteristics of aroyloxyl radicals. 1. The 4-methoxybenzoyloxyl radical. *J. Am. Chem. Soc.* **1988**, *110*, 2877−2885.

(6) Ingold, K.; Lusztyk, J.; Chateauneuf, J. Spectroscopic and kinetic characteristics of aroyloxyl radicals. 2. Benzoyloxyl and ring-substituted aroyloxyl radicals. *J. Am. Chem. Soc.* **1988**, *110*, 2886−2893.

(7) Yamauchi, S.; Hirota, N.; Takahara, S.; Misawa, H.; Sawabe, K.; Sakuragi, H.; Tokamaru, K. A time-resolved EPR study on photodecomposition of dibenzoyl peroxides in carbon tetrachloride. *J. Am Chem. Soc.* **1989**, *111*, 4402−4407.

(8) Abel, B.; Assmann, J.; Botschwina, P.; Buback, M.; Kling, M.; Oswald, R.; Schmatz, S.; Schroeder, J.; Witte, T. Experimental and theoretical investigations of the ultrafast photoinduced decomposition of organic peroxides in solution: Formation and decarboxylation of benzoyloxy radicals. *J. Phys. Chem. A* **2003**, *107*, 5157−5167.

(9) Abel, B.; Buback, M.; Kling, M.; Schmatz, S.; Schroeder, J. A seemingly well understood light-induced peroxide decarboxylation reaction reinvestigated with femtosecond time resolution. *J. Am Chem. Soc.* **2003**, *125*, 13274−13278.

(10) Buback, M.; Kling, M.; Schmatz, S.; Schroeder, J. Photo-induced decomposition of organic peroxides: Ultrafast formation and decrboxylation of carbonyloxy radicals. *Phys. Chem. Chem. Phys.* **2004**, *6*, 5441−5445.

(11) Kling, M.; Schmatz, S. Decarboxylation of carbonyloxy radicals: a density functional study. *Phys. Chem. Chem. Phys.* **2003**, *5*, 3891−3896.

(12) Charpentier, P. A.; DeSimone, J. M.; Roberts, G. W. Decomposition of Polymerisation Initiators in Supercritical CO2: A Novel Approach to Reaction Kinetics Using a CSTR. *Chem. Eng. Sci.* **2000**, *55*, 5341.

(13) Cohen, S. G.; Sparrow, D. B. Some reactions of diisopropyl peroxydicarbonate. *J. Am. Chem. Soc.* **1950**, *72*, 611−614.

(14) Kadla, J. F.; DeYoung, J. P.; DeSimone, J. M. The thermal decomposition of perfluoroalkyl peroxides in carbon dioxide. *Polym. Prepr. (Am. Chem. Soc., Div. Polym. Chem.*) **1998**, *39*, 835−836.

(15) Moller, C.; Plesset, M. S. Note on an approximation treatment for many-electron systems. *Phys. Rev.* **1934**, *46*, 618−622.

(16) Frisch, M. J.; Trucks, G. W.; Schlegel, H. B.; Scuseria, G. E.; Robb, M. A.; Cheeseman, J. R.; Montgomery, J. A.; Vreven, T.; Kudin, K. N.; Burant, J. C.; Millam, J. M.; Iyengar, S. S.; Tomasi, J.; Barone, V.; Mennucci, B.; Cossi, M.; Scalmani, G.; Rega, N.; Petersson, G. A.; Nakatsuji, H.; Hada, M.; Ehara, M.; Toyota, K.; Fukuda, R.; Hasegawa, J.; Ishida, M.; Nakajima, T.; Honda, Y.; Kitao, O.; Nakai, H.; Klene, M.; Li, X.; Knox, J. E.; Hratchian, H. P.; Cross, J. B.; Bakken, V.; Adamo, C.; Jaramillo, J.; Gomperts, R.; Stratmann, R. E.; Yazyev, O.; Austin, A. J.; Cammi, R.; Pomelli, C.; Ochterski, J. W.; Ayala, P. Y.; Morokuma, K.; Voth, G. A.; Salvador, P.; Dannenberg, J. J.; Zakrzewski, V. G.; Dapprich, S.; Daniels, A. D.; Strain, M. C.; Farkas, O.; Malick, D. K.; Rabuck, A. D.; Raghavachari, K.; Foresman, J. B.; Ortiz, J. V.; Cui, Q.; Baboul, A. G.; Clifford, S.; Cioslowski, J.; Stefanov, B. B.; Liu, G.; Liashenko, A.; Piskorz, P.; Komaromi, I.; Martin, R. L.; Fox, D. J.; Keith, T.; Al-Laham, M. A.; Peng, C. Y.; Nanayakkara, A.; Challacombe, M.; Gill, P. M. W.; Johnson, B.; Chen, W.; Wong, M. W.; Gonzalez, C.; Pople, J. A. *Gaussian03*, Revision C.02 ed.; Gaussian, Inc.: Wallingford, CT, 2004.

(17) Becke, A. D. Density-functional thermochemistry. III. The role of exact exchange. *J. Chem. Phys.* **1993**, *98*, 5648−5652.

(18) Lee, C.; Yang, W.; Parr, R. G. Development of the Colle-Salvetti correlation-energy formula into a functional of the electron density. *Phys. Rev. B* **1988**, *37*, 785−789.

(19) Head-Gordon, M.; Pople, J. A.; Frisch, M. J. MP2 energy evaluation by direct methods. *Chem. Phys. Lett.* **1988**, *153*, 503−506.

(20) Frisch, M. J.; Head-Gordon, M.; Pople, J. A. A direct MP2 gradient method. *Chem. Phys. Lett.* **1990**, *166*, 275−280.

(21) Frisch, M. J.; Head-Gordon, M.; Pople, J. A. Semidirect algorithms for the MP2 energy and gradient. *Chem. Phys. Lett.* **1990**, *166*, 281−289.

(22) Head-Gordon, M.; Head-Gordon, T. Analytic MP2 frequencies without fifth-order storage. Theory and application to bifurcated hydrogen bonds in the water hexamer. *Chem. Phys. Lett.* **1994**, *220*, 122−128.

(23) Gonzalez, C.; Schlegel, H. B. An improved algorithm for reaction-path following. *J. Chem Phys.* **1989**, *90*, 2154−2161.

(24) Gonzalez, C.; Schlegel, H. B. Reaction-path following in mass-weighted internal coordinates. *J. Phys. Chem.* **1990**, *94*, 5523−5527.

(25) Bunyard, C. W.; Kadla, J. F.; DeSimone, J. M. Viscosity effects on the thermal decomposition of bis(perfluoro-2-*N*-propoxypropionyl) peroxide in dense carbon dioxide and fluorinated solvents. *J. Am Chem. Soc.* **2001**, *123*, 7199−7206.

(26) Renbaum, A.; Szwarc, M. Kinetics of the thermal decomposition of diacetyl peroxide. I. Gaseous phase. *J. Am. Chem. Soc.* **1954**, *76*, 5975−5978.

(27) Levy, M.; Steinberg, M.; Szwarc, M. Kinetics of the thermal decomposition of diacetyl peroxide. II. Effects of solvents on the rate of the decomposition. *J. Am. Chem. Soc.* **1954**, *76*, 5978−5981.